

Investigation of Electrical Conduction Mechanism in Double-Layered Polymeric System

Prashant Shukla, M. S. Gaur

Department of Physics, Hindustan College of Science and Technology, Farah, Mathura, Uttar Pradesh, India

Received 14 June 2008; accepted 6 March 2009

DOI 10.1002/app.30443

Published online 2 June 2009 in Wiley InterScience (www.interscience.wiley.com).

ABSTRACT: The electrical conduction in solution-grown polymethylmethacrylate (PMMA), polyvinylidene fluoride (PVDF) and PMMA-PVDF double-layered samples in the sandwich configuration (metal-polymer-metal) was investigated at different fields in the range 100–120 kV/cm as a function of temperature in the range 293–423 K for samples of constant thickness of about 50 μm . Certain effects which lead to a large burst of current immediately after the application of field were observed in double-layered samples. An attempt was made to identify the nature of the current by comparing the observed dependence on electric field, electrode material and temperature with the respective characteristic features of the existing theories on electrical conduction. The observed linear I-V characteristics show that the electrical conduction follows Pool-Fren-

kel mechanism in PMMA and PVDF samples. Whereas, the non-linear behavior of current-voltage measurements in PMMA-PVDF double-layered samples have been interpreted on the basis of space charge limited conduction (SCLC) mechanism. The conductivity of the polymer films increased on formation of their double-layer laminates. The polymer-polymer interface act as charge carrier trapping centres and provides links between the polymer molecules in the amorphous region. The interfacial phenomenon in polymer-polymer heterogeneous system has been interpreted in terms of Maxwell-Wagner model. © 2009 Wiley Periodicals, Inc. *J Appl Polym Sci* 114: 222–230, 2009

Key words: amorphous; interfaces; activation energy; Maxwell-Wagner effect; electrical conduction

INTRODUCTION

The electrical conduction in polymers has much importance because of the discovery of the memory phenomenon¹ and has wide applications in thin film devices.² Most plastics are dielectrics or insulators and resist the flow of current. This is one of the most useful properties of plastics and makes much of our modern society possible through the use of plastics as wire coatings, switches, and other electrical and electronic products. Despite this, dielectric breakdown can occur at sufficiently high voltages to give current transmission and possible mechanical damage to the plastic.

In recent years, thin film technology is well established and is widely used in fabricating electronic devices. This technique has been successfully used to fabricate thin film resistors, capacitors, photoelectronic devices, etc. The use of this technique in fabricating electronic devices makes it necessary to understand the electrical properties of the material in the thin film form.³ This led to new discoveries in

the area of polymers that has now become one of the hot topics of research. Electrical properties constitute one of the most convenient and sensitive methods for studying the polymer structure.^{4,5} The interest in organic and polymeric semiconductors has arisen, particularly, because of their electrophotographic and solar cell applications.

In the case of organic solids, where the conductivity due to the electron exiting from the valence band to the conduction band^{6,7} is negligible, a complex conduction behaviour^{8,9} has been explained usually in terms of electron emission from the cathode i.e., Schottky–Richardson mechanism,¹⁰ or the electron liberation from traps in the bulk of the material i.e., Poole–Frenkel mechanism.¹¹ However, the possibility of tunneling¹² and space charge limited conduction has also been reported in the literature.¹³

The polymer composites receive much attention in terms of their mechanical and electrical properties, but the polymer multilayers receive relatively less attention in terms of their electrical conduction properties. Nevertheless, the electrical properties are relevant to the use of the layered polymer matrix for nonstructural purposes such as sensing and electromagnetic interference (EMI) shielding. The ability to provide nonstructural functions allows a structural material to be multifunctional, thus saving cost and enhancing durability. Furthermore, the electrical properties shed light on the structure of the

Correspondence to: M. S. Gaur (mulayamgaur@rediffmail.com).

Contract grant sponsor: Uttar Pradesh Council of Science and Technology, Lucknow.

materials, particularly concerning the interfaces in the layered polymers. Interfaces are often encountered in practical insulation systems, and have become a growing area of interest, because of their influence on the electrical performance of the whole system. Unlike the case of semiconductors, where transistors and diodes utilize characteristics of interfaces (p-n junctions), the interfaces in high electrically stressed materials, whether polymer or metal or polymer or polymer, can cause accumulation of space charge that can lead to unwanted electric field modification. It has been proposed¹⁴ that the accumulated space charge at the interface is a more significant factor with regard to the electric field enhancement than in the bulk. Despite of increasing interests in the interfaces, the underlying mechanisms related to charge formation and electrical ageing are not well understood, and research on the best interfacial materials and their binding structure is becoming increasingly important. Chen et al.¹⁵ have adopted a similar approach for the polymer-polymer interface where the interface is formed by laminating different polymers.

Therefore, for both technological and fundamental reasons, the electrical properties of the layered polymers are of interest and constitute the subject of investigation. This study addresses the measurement of the electrical conductivity on insulating polymers, such as PMMA, PVDF, and PMMA-PVDF double-layered samples, with varying temperature and field. We have tried to study the nature of the charge transport phenomenon and the conduction mechanism involved. An attempt is made to explore whether the double layer formation enhances or disrupts the conduction process.

EXPERIMENTAL

Sample preparation

The PVDF with weight-average molecular weight, $M_w = 2,61,000$ g/mol and density = 1.78 gm/cm³ is commercially available (Solvay Corporation, Brussels, Belgium) under the trade name Solef 1015 as a powder, and PMMA with $M_w = 145,000$ g/mol and density = 1.19 gm/cm³ was obtained from BDH, Poole, England. All samples were prepared using the solution grown technique. The solution of a particular concentration was prepared in a glass beaker by dissolving 50 mg PMMA in 100 mL of benzene and by dissolving 50 mg PVDF in 50 mL of dimethylformamide (DMF), separately at 50°C by using a teflon magnetic stirrer. The solution was then kept for 24 h at room temperature (30°C) to become homogeneous and transparent. The solution thus prepared was poured onto an optically plane glass plate floating on mercury pool; plates were with-

drawn from the mercury pool, and the solvent was then allowed to evaporate inside an oven at 40°C for 24 h, to yield the desired samples. Further, the dried samples were subjected to room temperature outgassing at 10^{-5} torr for a period of 24 h to remove any residual solvent. Polymer films are then gently peeled off from the glass plates. Thin films of the two polymers i.e., PMMA and PVDF were then compressed together under a compression moulding machine at a temperature of 65°C and a pressure of 2500 lbin⁻² (17.25 mPa) to yield double-layered samples with PMMA on one side and PVDF on the otherside.

Thickness measurement and electrode coating

The samples thus prepared, were like circular discs of 5-cm diameter and approximately 50- μ m thick, measured using a micrometer screw gauge with a least count of 0.001 cm. The dielectric constants for the PVDF, PMMA, and the PVDF-PMMA double-layered samples are equal to 7, 3.3, and 1.6, respectively calculated at 1 kHz and 300 K by measuring the capacitance using Agilent-Precision LCR meter (model: 4284A) with a similar (Al-Al) electrode combination, by using the relation given in the literature.¹⁶ Both the surfaces of the samples were vacuum aluminized using Hindhivac Vaccum coating unit with Penning and Pirani pressure gauges (model: ST-A6P3); over the central circular area of 3.5-cm diameter for the conductivity measurements.

Experimental procedure

Electrical conductivity of all polymer films is measured by a two-probe technique.¹⁷ The experimental set-up used for this study is shown in Figure 1. The metallized sample is sandwiched between the plates of the capacitor, which is made of aluminum, and a high dc voltage is applied across the two electrodes of the assembly by using a high dc voltage power supply (EHT-11, Scientific Equipments, Roorkee, India).

The assembly was placed inside a digitally controlled, thermally insulated oven (Ambassador, IBP,

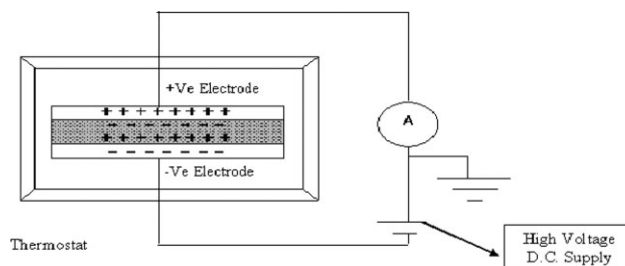


Figure 1 Schematic of the two-probe technique.

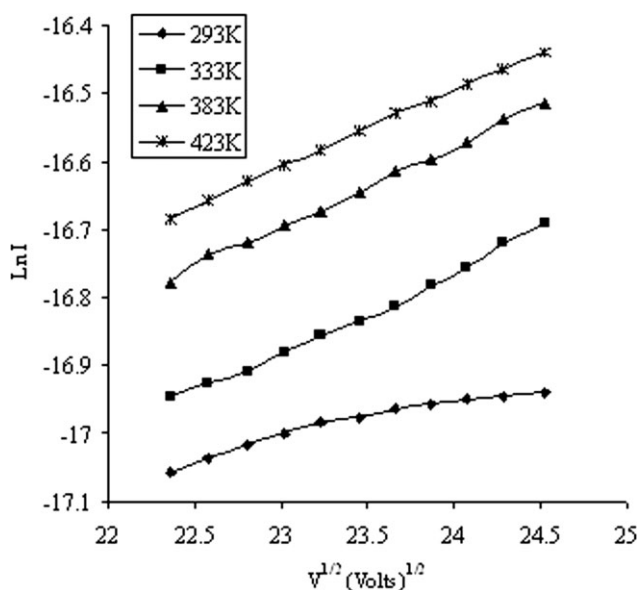


Figure 2 Plots of the $\text{Ln } I$ vs. $V^{1/2}$ (volt) $^{1/2}$ for PMMA samples.

India). The temperature of the oven is kept constant for a set of observations. A current is generated as a function of the applied voltage, which is measured with a sensitive digital electrometer (DPM-111, Scientific Equipments, Roorkee, India), which was carefully shielded and grounded to avoid ground loops or extraneous electrical noise. A coaxial-shielded cable was used to eliminate electric noise in case of low current measurements. The slope of the I - V characteristics gives the value of resistance of the polymer sample.

The volume resistivity (ρ) is a measure of the resistance of the material in terms of its volume. A voltage (≈ 500 V) is applied across the two electrodes, and the current is measured to allow calculation of the volume resistivity. The volume resistivity is calculated from the relation reported in the literature.¹⁸

RESULTS AND DISCUSSION

Current-voltage dependence

Current-voltage responses (plotted in the form of $\text{Ln } I$ - $V^{1/2}$ curves) for PMMA and PVDF samples exhibit linear relationship at different temperatures as shown in Figures 2 and 3, respectively. At low applied fields and temperatures, majority of the plots show slight deviations from this linear behavior. This deviation is, perhaps, due to the accumulation of space charges near the electrodes. The general trend of the slopes of the lines shows an increase as the applied fields and temperature increases. Thus, we conclude that the current flowing through the samples increases as the applied

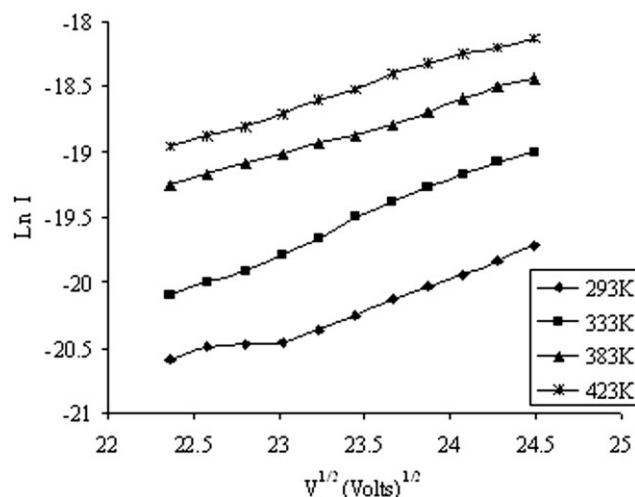


Figure 3 Plots of the $\text{Ln } I$ vs. $V^{1/2}$ (volt) $^{1/2}$ for PVDF samples.

field and temperature increases. Further, the curves exhibit a thermally activated conduction in the entire temperature range.

Figure 4 indicates the variation of current with the square root of the applied voltage for Al-film-Ag sandwich structure in the PMMA and PVDF samples, which is found to be independent of the polarities. This signifies that Poole-Frenkel mechanism governs the conduction process in the PMMA and PVDF samples.

Figure 5 shows the electrical conductivity versus temperature curves for PMMA and PVDF samples. Both the thermograms show a linear increase in the conductivity as the temperature is increased. Thus, we can say that the electrical conductivities for both PMMA and PVDF samples are strongly temperature dependent.

The current-voltage characteristics for the PMMA-PVDF double-layered samples as depicted by

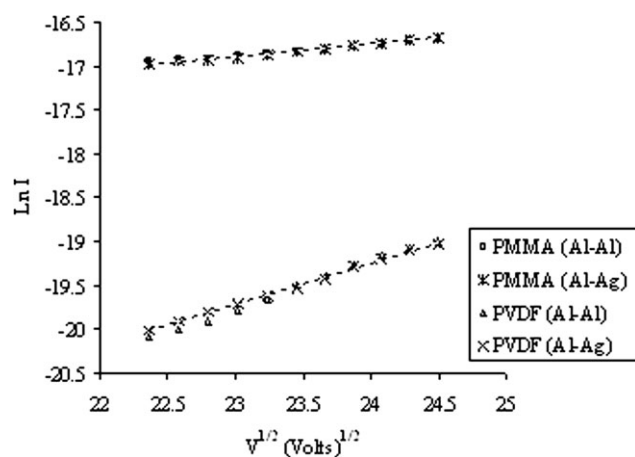


Figure 4 Variation of current with the square root of the applied voltage for an Al-film-Al and Al-film-Ag combination for PMMA and PVDF samples at 333 K.

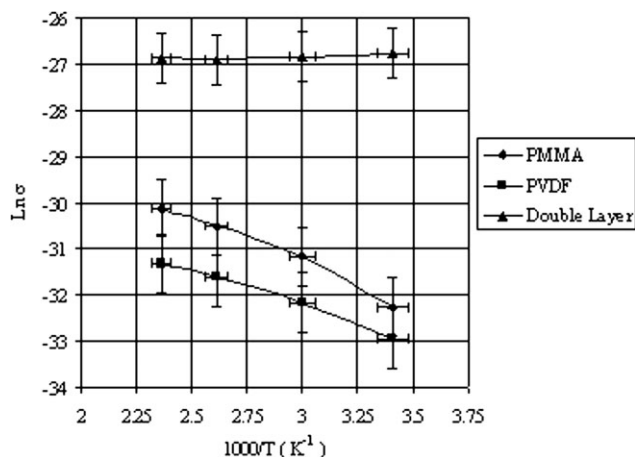


Figure 5 Temperature dependence of the DC conductivity in PMMA, PVDF, and PMMA-PVDF double-layered samples.

Figure 6 (plotted in the form of Log I-Log V curves) and Figure 7 (plotted in the form of Ln (I/V)-V curves) exhibit nonlinear relationship at different temperatures. The trend of the slopes of the lines shows a decrease as the temperature increases. Thus, we conclude that the current flowing through the sample decreases nonlinearly with an increase in the temperature.

Figure 5 shows the electrical conductivity versus temperature curve for the PMMA-PVDF double-layered samples. The thermograms show a linear decrease in the conductivity with an increase in the temperature, and then the conductivity increases gradually with the two different regions of conduction, with different slopes, giving rise to a knee at 383 K. Thus, we can say that the electrical conductivity for the PMMA-PVDF double-layered samples is also strongly temperature dependent.

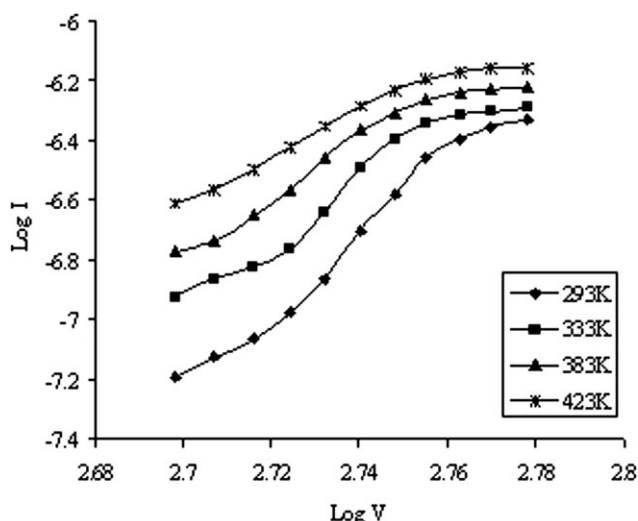


Figure 6 Plots of the Log I vs. Log V for the PMMA-PVDF double-layered samples.

Conduction mechanism

The current-voltage dependence exhibited by the plots at all temperatures, shown in Figures 2 and 3 is found to obey the following relation¹⁹

$$I \propto \exp\left(\frac{e\beta E^{1/2}}{kT}\right), \quad (1)$$

where E is the applied electric field, e is the electronic charge, β is a constant characteristic of the conduction mechanism, k is Boltzmann's constant, and T is the absolute temperature. The observed relation between the current and voltage, points to a conduction mechanism, in which, the charge carriers are released by thermal activation over a coulombic potential barrier that is decreased by the applied electric field. The potential barrier can be one of the two types: (i) barrier between electrodes and dielectric taking the classic image force into consideration (Schottky-Richardson Emission) and (ii) barriers due to trapping centers in the dielectric Pool-Frankel (PF) effect.²⁰

The linear behavior of the I-V characteristics points to an electronic-type conduction because of either the Schottky-Richardson (R-S) emission mechanism or the Poole-Frenkel (P-F) mechanism.

The expression for the current density according to Schottky emission is

$$J_{RS} = RT^2 \exp\left(\frac{-e\Phi_{RS}}{kT}\right) \exp\left[1/kT \left(\frac{e^3 E}{4\pi\epsilon\epsilon_0}\right)^{1/2}\right], \quad (2)$$

Where R is the Richardson constant, T is the absolute temperature, Φ_{RS} is the barrier height at the

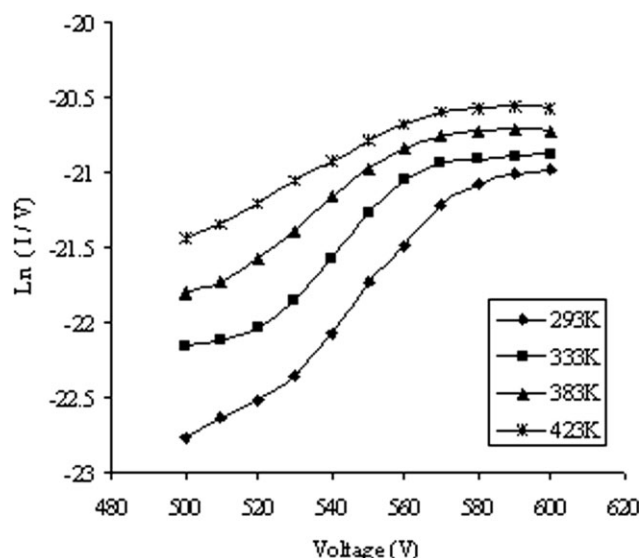


Figure 7 Plots of the Ln (I/V) vs. V (volt) for the PMMA-PVDF double-layered samples.

metal polymer interface in the absence of a field, e is the electronic charge, k is Boltzmann's constant, ϵ is the dielectric constant of the material, and ϵ_0 is the permittivity of free space. The expression for the current density according to Poole–Frenkel mechanism is

$$J_{\text{PF}} = cE \exp\left(\frac{-e\Phi_{\text{PF}}}{kT}\right) \exp\left[1/kT \left(e^3 E / \pi \epsilon \epsilon_0\right)^{1/2}\right] \quad (3)$$

where c is a constant, and $e\Phi_{\text{PF}}$ is the depth of the potential well.

To differentiate between these two mechanisms, the theoretical values of β were calculated for the Poole–Frenkel and Schottky mechanism

$$\beta_{\text{PF}} = \left(\frac{e}{kT}\right) \left(\frac{e}{\pi \epsilon \epsilon_0 d}\right)^{1/2}, \quad (4)$$

$$\beta_{\text{RS}} = \left(\frac{\beta_{\text{PF}}}{2}\right). \quad (5)$$

The values of dielectric constants for the PVDF and PMMA are substituted in eqs. (4) and (5), and the experimental values of β were calculated from the slopes of the $\ln I$ vs. $V^{1/2}$ plots as shown in Table I. The values of β increase, in most cases, as the temperature increases. These values are also generally larger than the theoretical values of β_{PF} and β_{RS} . Thus, the comparison between the theoretical and the experimental values of β does not reveal the mechanism which is involved in conduction in the case of the PMMA and PVDF samples.

The distinction between these two mechanisms depends upon the preexponential factors of eqs. (2) and (3) i.e., for Schottky mechanism and Poole–Frenkel mechanism, as shown by eqs. (6) and (7), respectively

$$J_{\text{ORS}} = RT^2 \exp\left(\frac{-e\Phi_{\text{RS}}}{kT}\right), \quad (6)$$

$$J_{\text{OPF}} = cE \exp\left(\frac{-e\Phi_{\text{PF}}}{kT}\right). \quad (7)$$

The Poole–Frenkel approach maintains the Schottky–Richardson formalism considering the barriers due to traps. If one takes an asymmetric metal–polymer–metal structure with two electrodes of different work functions, the current in the case of Schottky effect will be asymmetrical when polarities are reversed. But it remains practically unchanged in the case of Poole–Frenkel effect, because it does not depend upon the potential barriers at the interface as represented in Figure 4. This way of distinguishing the Poole–Frenkel and the Schottky–Richardson mechanism was suggested by Jonscher and Ansari.²¹ Thus, the effect of the nature of electrode materials of different work functions on the current–voltage characteristics has to be considered for deciding conduction mechanism.

The current–voltage characteristics for PMMA–PVDF double-layered samples as depicted in Figures 6 and 7 represents conduction regions with different slopes, which implies that the I–V relation is of the Type I $\propto V^{-n}$ where n is the slope of the curves. The current increases nonlinearly with the applied voltage and does not follow the power law, $I = kV^m$, where k and m are constants.²² The possibility of ohmic conduction is ruled out from the observed behaviour of I–V characteristics. This is also evident from the fact that Ohm's law follows from the free electron model of a metal. In the present study of PMMA–PVDF double-layered samples, polymers involved are, PMMA which is a polar, amorphous polymer, whereas PVDF is nonpolar, semicrystalline polymer. The individual polymer films are laminated one over the other to give rise to a heterogeneous system with polymer–polymer interface, and both the polymers are strong insulators with different characteristic properties and glass transition temperatures, giving wide scope for irregularities in the structure and so ruling out ohmic conduction.

TABLE I
Theoretical and Experimental Values of β and Slopes of Lines for PMMA and PVDF Samples

Material	T (K)	Slope ($\times 10^{-2}$)	β ($V^{-1/2} \text{ cm}^{1/2}$) $\times 10^{-4}$	$\beta_{\text{PF}} \times 10^{-4}$	$\beta_{\text{RS}} \times 10^{-4}$
PMMA	293	4.71	0.84	2.32	1.16
	333	11.79	2.39	2.04	1.02
	383	11.6	2.63	1.82	0.91
	423	11.42	2.72	1.76	0.83
PVDF	293	48.49	8.65	1.6	0.8
	333	58.3	11.82	1.4	0.7
	383	40.28	9.39	1.22	0.61
	423	42.83	11.03	1.1	0.55

The conductivity behavior of such films may be dominated by the properties of the amorphous regions.²³ Moreover, the semicrystalline polymer has crystalline lamellae, the remainder being amorphous material as reported by Florey.²⁴ In most heterogeneous polymeric systems, it is very difficult to observe any electronic conductivity, and if there is conductivity, it usually depends upon the movement of adventitious ions generated probably because of impurities centers in the lattice or impurities induced as a cause of experimental limitations.²⁵ Naturally, with a feeble charge carrier density, space charge limited conduction seems a remote possibility. Azad et al.²⁶ reported such a multilayer system on alumina substrates. He also reported an increase in the total ionic conductivity with an increasing number of interfaces, but did not specify the origin of this effect. He assumed that the lattice strain and the extended defects due to the lattice mismatch between the two adjacent phases might be responsible for ionic conductivity.

Ionic conduction consists of a transit of ions (atoms of positive or negative charge) from one site to another through point defects (vacancies) in the lattice structure. At normal ambient temperatures, very little ion hopping takes place, because the atoms are at relatively low energy states. At high temperatures, however, vacancies become mobile, and certain materials exhibit ionic conduction.²⁷ There are certain materials which have compact crystalline or amorphous structure, and ion displacement is only possible because of point defects as vacancies or interstitial ions. This process can lead to the transport of ions across the solid, giving rise to conductivity. This mechanism is termed as vacancy migration.²⁸ These materials present an intrinsic conduction, associated with the concentration of defects of thermal origin, Frenkel or Schottky disorder, and an extrinsic conduction, associated with the concentration of point in the ionic or cationic sublattice created by impurities. Intrinsic and extrinsic conduction are both characterized by the activation energy. The intrinsic conduction activation energy is always high since it involves two terms: one representing the energy needed to form a point defect, and second, the migration energy of this defect. In the extrinsic domain, at lower temperature, the activation energy is lower, because it reflects only the migration energy. The value of 1 eV often constitutes a boundary between the two types of conduction.^{27–29}

The conduction mechanism, which gives rise to the nonlinear current-voltage characteristics, is the space charge limited conduction (SCLC)³⁰ which is influenced by traps. The defects and impurities can govern the conduction mechanism and also act as trapping centers, and get populated by the injected charge carriers from the electrodes. However, the

exact nature of the traps present in the double-layered polymeric heterogeneous system under study depends on the type of the traps and their position, with respect to the Fermi-level.

The space charge limited currents may also determine the behaviour, which leads to a large burst of current immediately after the application of voltage followed by a steady decline in current on standing. In the present case, the large currents obtained immediately after the application of voltage subsided to much smaller steady values after a certain length of time. The possible explanation is that the sudden application of voltage causes a cloud of carriers, i.e., a space charge, to be injected from the contact into the sample. This free charge gives rise to a large burst of current. If the space charge remained untrapped, the value of the transient current would continue as a steady current. However, one must take into account the effects of trap densities in the sample. The free charge forced into the sample settles, the rate being determined by the capture cross section of traps for free carriers.³¹ These injected carriers can easily pass through the PMMA-PVDF interface and move in the PMMA or PVDF region. This process increases the conductivity of the double-layered samples. The conductivity behaviour of such films may be dominated by the properties of the amorphous regions.²³ The polymer-polymer interface in the double-layered samples is supposed to create localized states of various depths, which will lead to trapping sites distributed over a considerably wide energy range. Because there are many localized states, the release or excitation of the carriers in these states dominates the conduction process. These localised states act as carrier trapping centres, and after trapping the injected charge from electrodes they become charged and are thereby expected to build up a space charge. This build up of space charge plays the key role in the determination of the SCLC process. The formation of interface is considered to reduce the barrier between the trapping sites, providing a conducting path through the polymer matrix, and would result in the enhancement of electrical conductivity with the increase in temperature.

The interfacial phenomenon in the double-layered polymeric system has been interpreted in terms of the Maxwell-Wagner model. However, the appearance of the additional trapping sites in the double-layered heterogeneous system could not be explained on the basis of this simple model. The interfacial phenomenon can be used to understand the injection of charge carriers from anode into the PMMA or PVDF region. This phenomenon is supposed to decrease the activation energy of the carrier and increase its mobility towards the electrode during polarization. The increase in current with the formation of double layer is supposed to lead to the

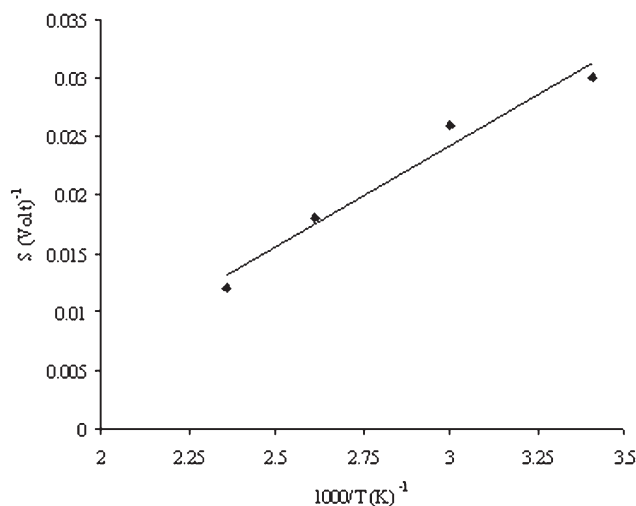


Figure 8 Plots of slope S of $\ln(I/V)$ as a function of V (volt) curves against $1000/T$ (K)⁻¹ for the PMMA-PVDF double-layered samples.

accumulation of more and more positive charge in front of the cathode, resulting in an increased strength of space charge at the polymer–electrode interface. Although, Maxwell–Wagner Interfacial polarization is not the dominating mechanism to describe the electrical conductivity and charge transport processes in the PVDF-PMMA double-layered samples, but since the heterogeneous system discussed in the present study has two layers with different permittivities and conductivities thus, there may be an effect due to the Maxwell–Wagner type interfacial polarization, which cannot be neglected.

The attribution to the SCL conduction is further supported by the following observation. (i) PMMA being an amorphous material, would provide a large number of trapping centres, and trapping of charge carriers in these trapping sites would result in the build-up of a space charge, (ii) PVDF is a semicrystalline polymer, thus charge trapping takes place at the molecular chain, the side chain, and at the interface of the crystalline and amorphous regions of the polymer,³² and (iii) the formation of polymer–polymer interface in the double-layered samples gives rise to additional molecular sites for trapping of charge carriers.³³ Such localized sites can be defined in molecular terms using the difference in ionization potential as an indication of trap depth. Blinov et al.³⁴ reported that during polarization, on application of high electric field in the double-layered samples, the charge carriers are accumulated within the vicinity of the interface, so that the local electric field in the interface is found to increase. This local electric field allows the movement of charge carriers through the interface during application of external voltage.

The temperature dependence of the current density, J for SCLC is given by,³⁵

$$J = en_0\mu F \exp\left(\frac{F\varepsilon_0\varepsilon}{eN_t kTd}\right), \quad (8)$$

where J is the current density for SCLC, d is the thickness of the film, μ is the mobility of the carriers, V is the applied voltage, F , the electric field = V/d , N_t is the trap density, and T is the absolute temperature.

eq. (8) can be rewritten as,

$$\frac{J}{V} = \left(\frac{en_0\mu}{S}\right) \exp\left(\frac{V\varepsilon_0\varepsilon}{eN_t kTd^2}\right). \quad (9)$$

$$\text{Therefore } \frac{J}{V} = A_0 \exp\left(\frac{V}{V_0}\right), \quad (10)$$

$$A_0 = \frac{en_0\mu}{d}, \quad (11)$$

$$V_0 = \frac{eN_t kTd^2}{\varepsilon_0\varepsilon}. \quad (12)$$

Thus, a plot of $\ln(I/V)$ vs. V should yield a straight line with slope $(1/V_0)$ and intercept A_0 . It is seen from Figure 7 that, the slopes of the curves decrease slightly with an increase in the temperature, as revealed from Figure 8. The decrease in slope $(1/V_0)$ with temperature implies that the Rose model¹³ that predicts the nature of trap distribution can be applied in the present study. These results indicated that the presence of space charge limited the conduction in all the double-layered samples. Using eq. (12) and plot of the slopes of $\ln(I/V)$ vs. V curves as shown in Figure 8, trap densities for various temperatures are computed. It is seen that the trap densities of the order of $10^{19} \text{ m}^3\text{eV}^{-1}$ exist for the present system and increases with increase in temperature as shown in Figure 9. These values are

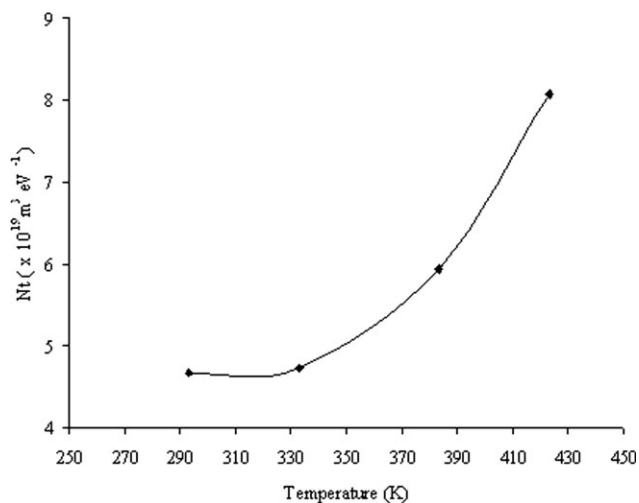


Figure 9 Plots of the trap charge density N_t ($\times 10^{19} \text{ m}^3 \text{eV}^{-1}$) vs. T (K) for PMMA-PVDF double-layered samples.

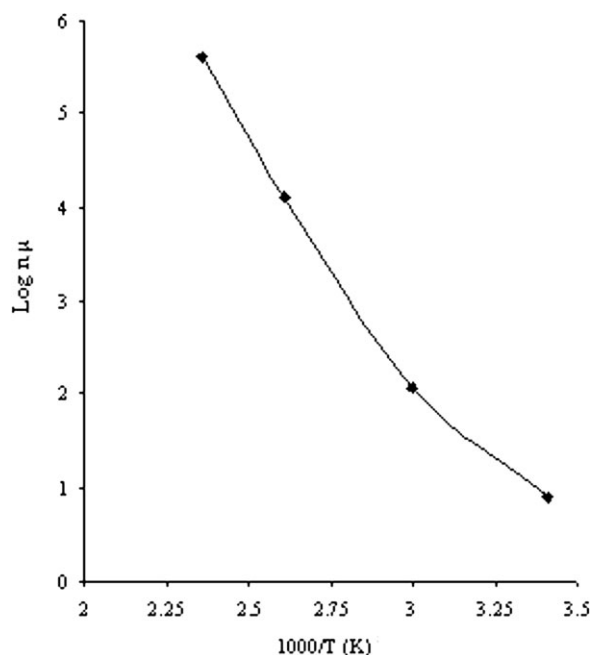


Figure 10 $\text{Log } (n_0\mu)-1000/T \text{ (K)}^{-1}$ characteristics for the PMMA-PVDF double-layered samples.

in close agreement with that reported for the similar disorder polymeric system.^{36,37}

It is further seen that using eq. (11) and the slope $(1/V_0)$ at different temperatures the values for $n_0\mu$ can be calculated. The intercept, $\log A_0$, is also found to be a function of the mobility μ of carriers, free electron density, and thickness of the sample. The mobility of carriers in glassy materials exhibits a trap activated temperature relation of the form,³⁸

$$\mu = \mu_0 \exp\left(\frac{E_t}{kT}\right), \quad (13)$$

where E_t is the activation energy of the traps eq. (13) can be rewritten as

$$n_0\mu = n_0\mu_0 \exp\left(\frac{E_t}{kT}\right). \quad (14)$$

Thus, it is possible to extract information about the activation energy of the traps (E_t) by plotting $\log n_0\mu$ vs. $1000/T \text{ (K)}^{-1}$ as depicted in Figure 10. It is seen that the plot is linear and, from the slope, the value of E_t is calculated to be 1.03 eV. This value is in close agreement with the one reported for a similar type of polymeric layered system.³⁹ The distribution of the traps in the sample could be either discrete or exponential. Rose¹³ gives the current voltage relation, which is in the form $I \propto V [(T_c/T) + 1]$, where T_c is the characteristic temperature. Thus $[(T_c/T) + 1]$ is the slope of the curves of Figure 6, which gives the T_c as 541 K. Thus, kT_c becomes 0.046

eV, which is very small compared with the average activation energy of the traps, determined as 1.03 eV. This suggests that the distribution of traps is uniform, which is expected for disordered amorphous or polycrystalline polymeric samples.¹³

Activation energy measurement

The dependence of the electrical conductivity σ for PMMA, PVDF, and PMMA-PVDF double-layered samples on temperature is depicted in Figure 5. It shows that σ is given by:

$$\sigma = \sigma_0 \exp\left(\frac{-E_{ac}}{kT}\right), \quad (15)$$

where σ_0 is the maximum conductivity and E_{ac} is the activation energy. The E_{ac} for the PMMA and PVDF sample is found to be 0.741 and 0.697 eV, respectively, which is typical of the electronic conduction.⁴⁰ This provides another support for our previous conclusion.

It is not possible to give definite limits for activation energy, but Jonscher and Ansari²¹ suggested that values less than 0.8 eV would normally be considered as the electronic conduction mechanism, whereas values in excess of 0.8 eV would normally be attributed to ionic transport.

The E_{ac} for PMMA-PVDF double-layered sample is found to be 1.028 eV, which suggest that ionic transport mechanism governs the conduction process in double-layered samples.

CONCLUSION

PMMA-PVDF double-layered samples show better conductivity in comparison with that of individual polymers. The dominant conduction mechanism in double-layered samples is identified as SCLC mechanism whereas P-F is the governing mechanism in PMMA and PVDF. It is further shown that the traps in the double-layered samples are distributed uniformly in the forbidden energy band-gap, as evident from the average activation energy of the traps determined as 1.03 eV. The activation energy for double-layered samples is found to be 1.028 eV, which is typical of ionic transport-dependent conduction mechanism.

References

1. Kryezewski, M. *Polym Sci Polym Symp* 1975, 50, 359.
2. Mead, C. A. *J Appl Phys* 1961, 33, 646.
3. Mott, N. F.; Davis, E. A. *Electronic Process in Non-Crystalline Materials*, 2nd ed.; Clarendon Press: Oxford, 1978.
4. Ferraro, J. R.; Walker, A. *J Chem Phys* 1965, 42, 1273.
5. Kimura, T.; Kajiwara, M. *J Mater Sci* 1998, 33, 2955.
6. Keton, J. E., Ed. *Organic Semiconducting Polymers*; Marcel Dekker: New York, 1968; p 267.

7. Khare, P. K.; Shrivastava, A. P. *Indian J Pure Appl Phys* 1991, 29, 1410.
8. Parak, N. C.; Garg, T. C. *Indian J Pure Appl Phys* 1991, 25, 110.
9. Khare, P. K. *Indian J Pure Appl Phys* 1994, 32, 160.
10. Schottky, W. *Z Phys* 1914, 15, 872.
11. Frenkel, J. *Phys Rev* 1938, 54, 647.
12. Fowler, R. H.; Nordheim, L. *Proc R Soc London Ser A* 1928, 119, 173.
13. Rose, A. *Phys Rev* 1955, 79, 1538.
14. Li, Y.; Takada, T.; Miyata, H.; Niwa, T. *J Appl Phys* 1993, 74, 2725.
15. Chen, G.; Brown, M. A.; Davies, A. E.; Rochester, C.; Doble, I. In the 9th International Symposium on Electret; Shanghai, China, 1996; p 285.
16. Akram, M.; Javed, A.; Rizvi, T. Z. *Turk J Phys* 2005, 29, 355.
17. Ashour, A. H.; Saad, H. M.; Ibrahim, M. M. *Egypt J Solids* 2006, 29, 351.
18. ASTM. ASTM Standard D 257, Standard method for DC resistance of conductance of insulating materials, Annual Book of ASTM Standards; American Society of Testing Materials: Philadelphia, 1993, Vol. 10.01, p. 103.
19. El Tayyan, A. A.; Khogali, A. *Chin J Phys* 2004, 42, 392.
20. Khare, P. K.; Gaur, M. S.; Srivastava, A. P. *Indian J Pure Appl Phys* 1994, 32, 14.
21. Jonscher, A. K.; Ansari, A. A. *Phil Mag* 1971, 23, 205.
22. Deshmukh, S. H.; Burghate, D. K.; Akhare, V. P.; Deogaonkar, V. S.; Deshmukh, P. T.; Deshmukh, M. S. *Bull Mater Sci* 2007, 30, 51.
23. Kosaki, M.; Yoda, M.; Ieda, M. *J Phys Soc Jpn* 1971, 31, 598.
24. Florey, P. J. *Principles of Polymer Chemistry*; Cornell University Press: Ithaca, New York, 1953.
25. Seanor, D. A. *Electrical Properties of Polymers*; Academic Press: 1982; p 19.
26. Azad, S.; Marina, O. A.; Wang, C. M.; Saraf, L.; Shutthanandan, V.; Mccready, D. E.; El-Azab, A.; Jaffe, J. E.; Engelhard, M. H.; Peden, C. H. F.; Thevuthasan, S. *Appl Phys Lett* 2005, 86, 131906/1.
27. Ionic conduction. In *Encyclopædia Britannica*. Available at: <http://www.britannica.com/EBchecked/topic/292965/ionic-conduction>. Accessed on 10th October 2008.
28. Padma Kumar, P.; Yashonath, S. *J Chem Sci* 2006, 118, 135.
29. Souquet, J. L. *Ann Rev Mater Sci* 1981, 11, 211.
30. Lampert, M. A.; Mark, P. *Current Injections In Solids*; Academic Press: New York and London, Ch. 4, 1970.
31. Singh, R.; Srivastava, A. P. *Indian J Pure Appl Phys* 1972, 10, 811.
32. Khare, P. K.; Gaur, M. S.; Singh, R. *Indian J Phys* 1994, 68A, 545.
33. Jonscher, A. K. *Thin Solid Films* 1967, 1, 213.
34. Blinov, L. M.; Palto, S. P.; Tevesov, A. A.; Barnik, M. I.; Weyrauch, T.; Haase, W. *Mol Mater* 1995, 5, 311.
35. Lampert, M. A.; Mark, P. *Current Injections In Solids*; Academic Press: NY, 1970.
36. Bodhane, S. P.; Shirodkar, V. S. *J Appl Polym Sci* 1999, 74, 1347.
37. Budinas, T.; Mackus, P.; Smilga, A.; Vivvakas, J. *Phys Solid State* 1969, 31, 375.
38. Solomon, I.; Benferhat, R.; Tran-Quoc, H. *Phys Rev* 1984, 30, 3422.
39. Kenshiro, N.; Kwan, C. K. *Jpn Appl Phys* 1979, 18, 1161.
40. Mort, J.; Pfister, G.; Sessler, G. M. *Electronic Properties of Polymers*; Mort, J.; Pfister, G., Eds.; Wiley: New York, 1982, p 109–160.